Supplemental Information: 3D Printed Device Methodology for Combined Thermal and Fluorescence Analysis

Derek Sanchez[1], Robert Macdonald[1], Brendan Mitchell[1], Marshall Rawlins[2], Jansen Engelbrecht[3], Gregory P. Nordin[2], Adam T. Woolley[3], Troy R. Munro[1*]

[1]Department of Mechanical Engineering, Brigham Young University, 350 Engineering Building, Provo, 84602, Utah, USA.
[2]Department of Electrical and Computer Engineering, Brigham Young University, 450 Engineering Building, Provo, 84602, Utah, USA.
[3]Department of Chemistry and Biochemistry, Brigham Young University, C100 BNSN, Provo, 84602, Utah, USA.

*Corresponding author(s). E-mail(s): troy.munro@byu.edu;

1 MCA Tesing on Commercial Instrument

The results of MCA using the QuantStudio 5 system are presented in Fig. 1. The three genotypes possible were tested: mutant homozygous, wild-type homozygous, and heterozygous. The three genotypes are presented with a different line style for each genotype. The QuantStudio 5 system performed PCR and then a melt curve analysis on the samples, heating them at a constant temperature rate and recording the fluorescence of the SYBR. The raw data for this is presented in Fig. 1a using the system's arbitrary relative fluorescent units (RFU) and reported temperature for each of the wells used. The portion of interest for sample analysis is the steep change near 81 $^{\circ}C$. This view gives us the expected MCA curve shape.

The simplest analysis of MCA data is done by taking the derivative of the RFU with respect to the temperature. Fig. 1b presents this derivative based on the raw RFU data of the system. For clarity, these derivatives are normalized, each by their maximum value and presented in Fig. 1c. Ideally, all of the mutant homozygous samples would be grouped together, separate from the wild-type homozygous samples,

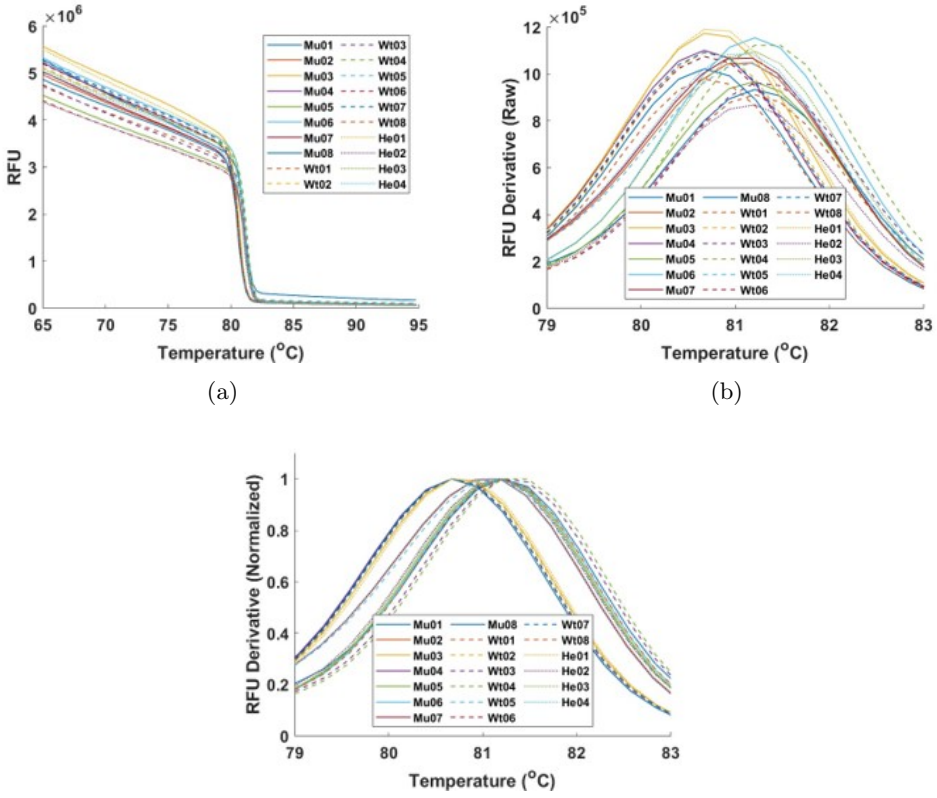

Fig. 1: Data from the QuantStudio 5 qPCR machine on FVL: WT/WT, Mu/Mu, and WT/Mu. (a) The raw melt curve data. (b) The quickest method of finding the melting temperature through calculating the first derivative of the raw data. (c) The derivatives normalized by each sample to try to group the genotypes.

and the heterozygous samples would have two distinct peaks. In this figure, all three genotypes are overlapping.

2 Experimental setup

Fig. 2 provides an image of the experimental setup used during fluorescence measurements. The entire setup is enclosed in a box to limit convective currents from the HVAC system within the research lab. The clear tubes coming from the MCA-mimicking device are filled with galinstan that is pressurized using a weight on a vertically oriented syringe. The black and yellow alligator clips are connected to a computer controlled power supply.

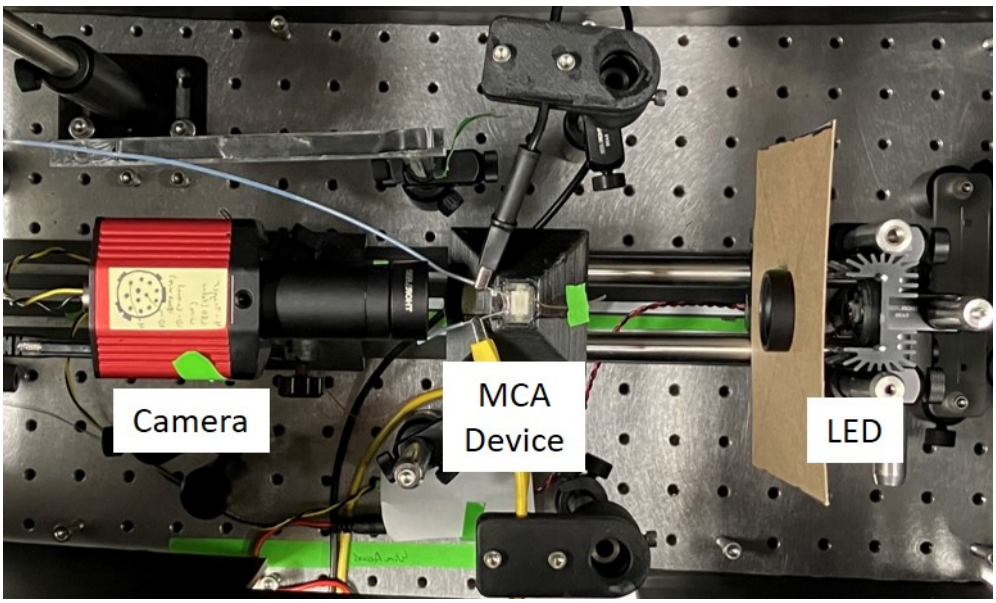

Fig. 2: Experimental setup image showing the key optical components used to measure fluorescence of the MCA-mimicking device.

3 Device Design

To ensure that thermal modeling of the microfluidic device was consistent, the device was printed is such a way that it could be removed from the glass slide it was printed on. This was made possible through the use of removable build supports shown in Figure 3.

A device holder, Fig. 4, was also build so that the airflow around the MCA-mimicking device would be consistent. It was split into two sections to allow easy placement and removal of devices. The two parts were held together by small magnets glued into small recesses and had two pegs to act as guides when closing the holder. The holder also featured four overhangs, one on each corner, that would fit over the SLA printed device corners and hold it in place. Under the device was a hollow column with a through hole that fit a 1/4"-20 screw for attachment to the optical setup.

4 Modeling

Material properties were assigned as follows. The bulk of the device was assigned as PEGDA, the glass slides were assigned as silica glass, the inlet needles were assigned as stainless steel 304, the heating channels were assigned as galinstan, the DNA sample was assigned as water, the device holder was assigned as polylactic acid (PLA), the thermocouple wire was assigned as chromel, and the surrounding cylinder was assigned as air (see Fig. 5). The PEGDA material and galinstan material were custom defined because the COMSOL material library did not contain them. An investigation into the

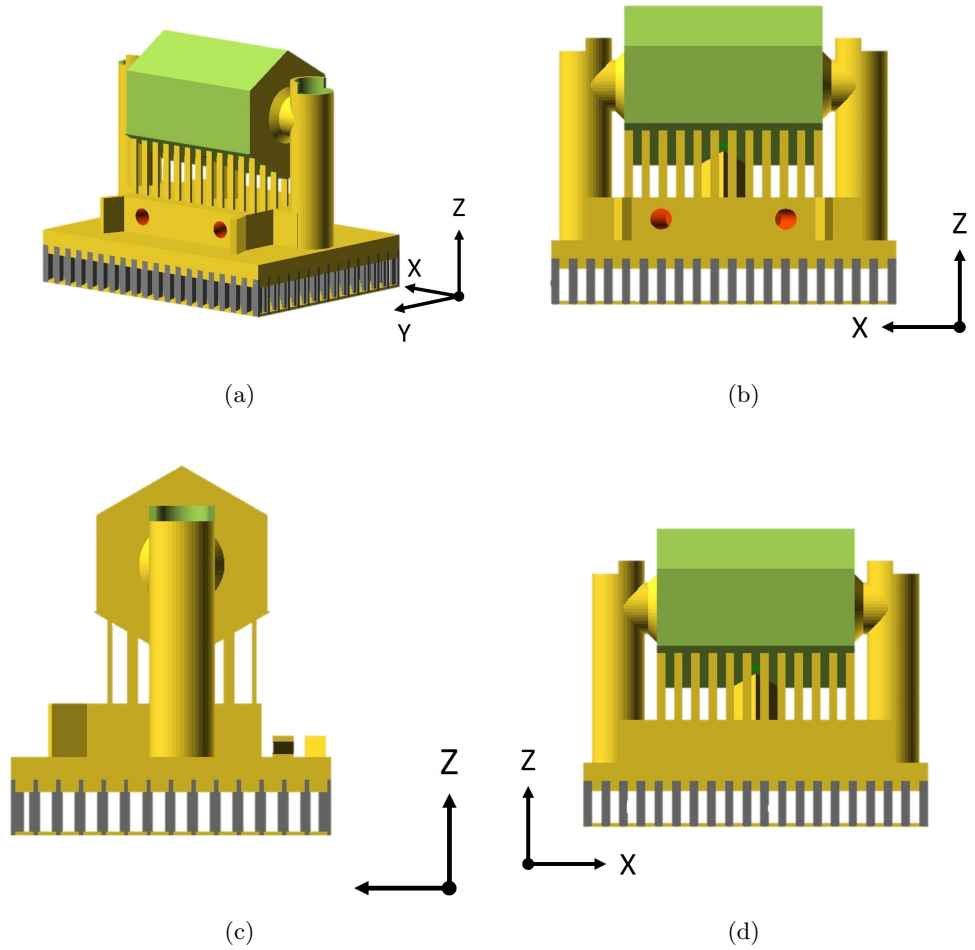

Fig. 3: The rendered printing file for the final MCA-mimicking device design. To successfully print the device, support columns are added into all the designed gaps and below the base. These support columns are removed after printing. (a) An isometric view. (b) A front view. (c) A side view. (d) A back view.

thermal properties of PEGDA was conducted, and the values found from this investigation were used in the COMSOL model. A heat capacity of $785\,J\,kg^{-1}\,K^{-1}$, a density of $1145\,kg\,m^{-3}$, and a thermal conductivity of $0.275\,W\,m^{-1}\,K^{-1}$ were used to model the PEGDA. The galinstan was assigned a thermal conductivity of $16.5\,W\,m^{-1}\,K^{-1}$, a heat capacity of $295\,J\,kg^{-1}\,K^{-1}$, and a density of $6440\,kg\,m^{-3}$; Khoshmanesh et al. (2017).

The electrical conductivity of galinstan was calculated from electrical resistivity measurements from literature Zhang et al. (2013); Shan et al. (2013). The relative permittivity of the galinstan did not affect the model, but a value of 12.9 was used to

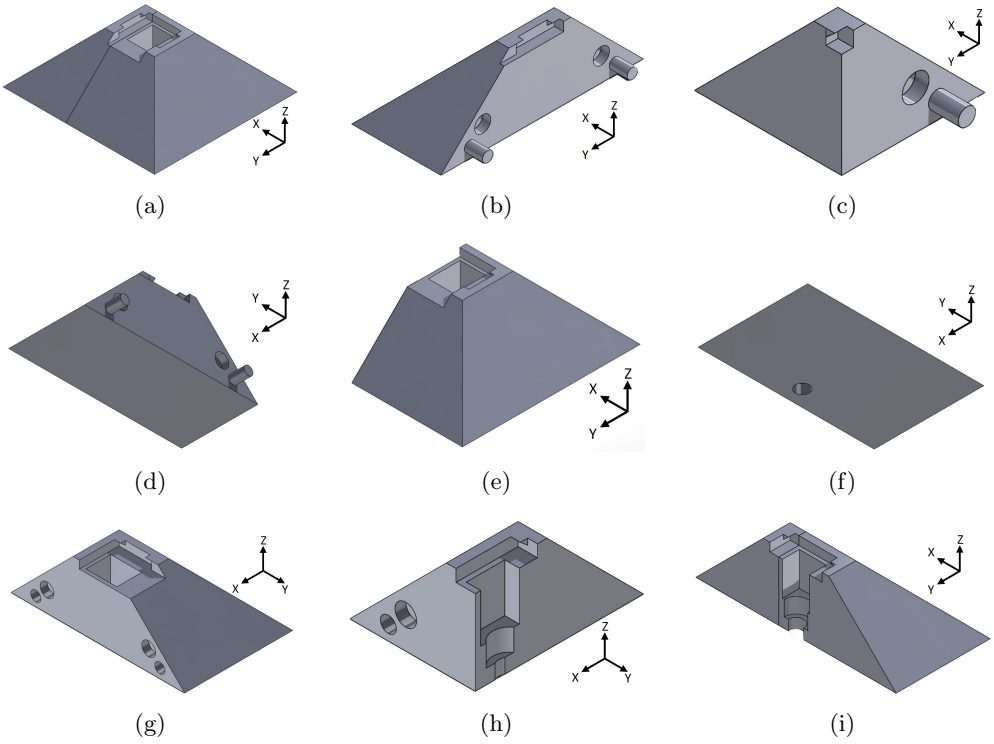

Fig. 4: One important consideration of the COMSOL model is the air flow around the device. A custom MCA-mimicking device holder was designed to hold the device in optical alignment with the optics and to normalize the convective airflow around the device.

be consistent with prior models Sanchez et al. (2022). Only the galinstan and needles were modeled as electrically conductive. A ground condition was added to one of the outer cylindrical faces of the needles, while the outer face of the other needle was modeled as a current source.

For fluid flow, all external faces of the cylindrical volume of air were modeled as fluid inlets, except for the base of the cylinder. The boundary condition for these inlets was chosen to be a pressure constraint of 0 Pa with backflow allowed.

References

Khoshmanesh, K., Tang, S.-Y., Zhu, J.Y., Schaefer, S., Mitchell, A., Kalantar-zadeh, K., Dickey, M.D.: Liquid metal enabled microfluidics. Lab on a Chip **17**, 974–993 (2017) https://doi.org/10.1039/C7LC00046D

Low Melting Point Alloy Galinstan - 68.5% Ga, 21.5% In, 10% Sn. https://www.rotometals.com/low-melting-point-alloy\

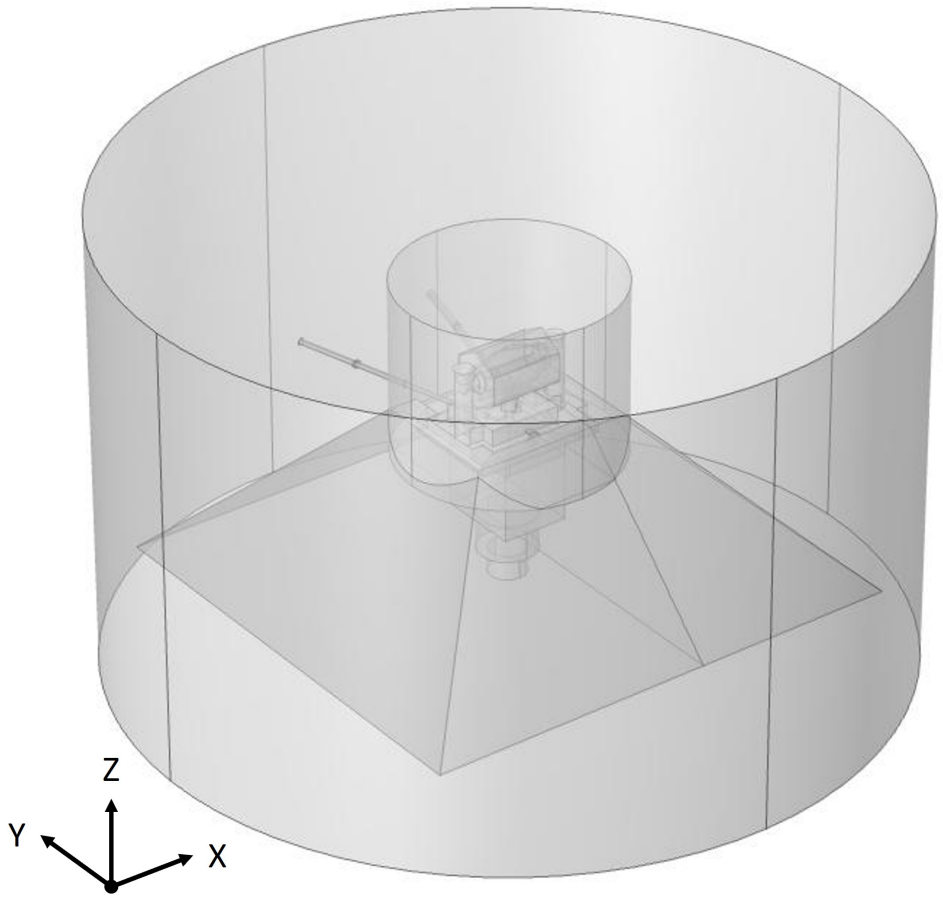

Fig. 5: The domains modeled in COMSOL. This includes the MCA-mimicking device, the steel tubes for the liquid metal electrical connection, the internal liquid metal, the internal water-suspended DNA sample, the device holder, the device holder insulation, and a column of surrounding air.

-galinstan-68-5-ga-21-5-in-10-sn-50-grams/

Sanchez, D., Hawkins, G., Hinnen, H.S., Day, A., Woolley, A.T., Nordin, G.P., Munro, T.: 3d printing-enabled uniform temperature distributions in microfluidic devices. Lab on a Chip **22**, 4393–4408 (2022) https://doi.org/10.1039/D2LC00612J

Shan, W., Lu, T., Majidi, C.: Soft-matter composites with electrically tunable elastic rigidity. Smart Materials and Structures **22**(8), 085005 (2013) https://doi.org/10.1088/0964-1726/22/8/085005

Zhang, B., Dong, Q., Korman, C.E., Li, Z., Zaghloul, M.E.: Flexible packaging and

integration of CMOS IC with elastomeric microfluidics. In: Allee, D.R., Forsythe, E.W. (eds.) Flexible Electronics, p. 873004 (2013). https://doi.org/10.1117/12.2015554